HERON contains contributions based mainly on research work performed in I.B.B.C. and STEVIN and related to strength of materials and structures and materials science.

Jointly edited by:

STEVIN-LABORATORY
of the Department of
Civil Engineering of the
Delft University of Technology,
Delft, The Netherlands
and
I.B.B.C. INSTITUTE TNO
for Building Materials
and Building Structures,
Rijswijk (ZH), The Netherlands.

Secretary:

G. J. van Alphen
Stevinweg 1
P.O. Box 5048
2600 GA Delft, The Netherlands

HERON vol. 24 1979 no. 4

Contents

Publications in HERON since 1970

Experiments on concrete beams reinforced with conventional reinforcement and steel fibres subjected to fatigue loading

Ir. H. A. Körmeling

1 Introduction

Structures submitted to dynamic loading have always invited special attention from the building engineer. It is presumable that with regard to a static loaded construction, a cyclic loading will increase some important design parameters such as deflection and crack width. In practice both values must be limited according the design codes. Although the precise nature of such increase is not known and the method to calculate these quantities, is not available, it is likely that the addition of steel fibres will reduce the crack widths and the deflections under fatigue loading. Of course alternative methods can be used to reduce the above mentioned parameters, such as higher reinforcement ratios.

The objective of the research reported here was to study the influence of steel fibres on the fatigue behaviour of conventionally reinforced concrete beams, this in respect to deflections, crack widths and crack distances.

2 Experimental investigation

A total amount of 15 concrete beams were tested in a four point dynamic loading test. The measurements were restricted to the constant moment zone and enclose midspan and loading point deflections, surface strain measurements at the top and bottom side of the specimen, crack widths and crack distances at reinforcement bar level.

The beams were 100 mm wide, 152 mm deep and 2200 mm long. The span was 2000 mm and the constant moment zone was 800 mm.

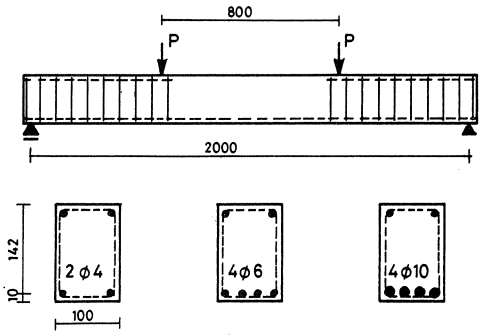

Fig. 1. Reinforcement details.

The concrete quality was B 42.5 (NEN 3861) with portland A cement and a maximum grain size of 16 mm. The conventional reinforcement consisted of continuous deformed bars (Hi Bond, yield stress = 500 N/mm^2) with diameters of 4, 6 or 10 mm. Three different reinforcement ratios of 0.17, 0.75 and 2.09% were provided by using 2 bars of 4 mm diameter, 4 bars of 6 mm diameter or 4 bars of 10 mm diameter, respectively. For reinforcement details see Fig. 1.

For each ratio, beams were made with concrete containing either no fibres or three different types of fibres shown in Fig. 2. The volume percentages of the straight fibres, the fibres with hooks and the fibres with paddles were 1.41, 0.89 and 1.53%, respectively. Owing to the different shapes and dimensions these volume percentages resulted in concrete with more or less the same workability. The scope of the test program can be seen in Table A1 of the Appendix.

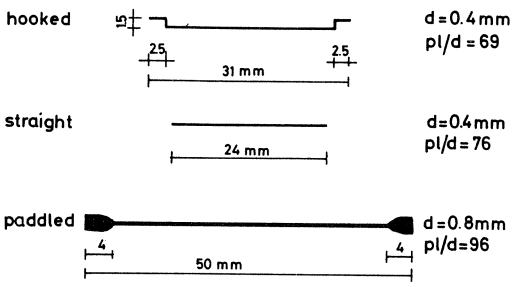

Fig. 2. Fibre types.

3 Testing equipment and instrumentation

The dynamic loading frame was specially designed to enable simultaneous testing of four different beams with only one pulsator.

Two hydraulic jacks were connected with the pulsator. By altering the position of the jacks between two test beams each beam could be loaded with the appropriate load. The load of each beam was measured through a load cell. The frequency of loading was 3 Hz.

For dynamic loading, the measurements were made after 1, 10, 100, 1000, 10.000, 50.000 and 100.000 and then every 100.000 cycles up to about one million cycles. Measurements were also made at the beginning and the end of the working day.

The deflections were measured near the load points and at the center with dial gages having a scale graduation of 0.01 mm. The strains on the top and bottom of the beams were measured by extensometers (containing electric resistance strain gages) attached to glued points on the top and bottom surfaces of the beam.

For dynamic loading, 3 extensometers were fixed at the top with gage lengths of 100, 150 and 100 mm, respectively, and 3 at the bottom surface with a gage length of 100 mm. To aid in crack detection, beams were whitewashed. Crack widths were measured with an illuminiated microscope with a scale division of 0.01 mm.

The crack widths were measured on one side of the beam at a distance of 10 mm from the bottom surface. This was the location of continuous rebars. Cracks were marked with black lines after each loading step. At the end of the test the beams were photographed.

4 Results of the dynamic tests

From the three groups of beams ($\rho = 0.17, 0.75, 2.09\%$) subjected to fatigue loading, the course of deflection and crack width values related to the number of loading cycles will be given.

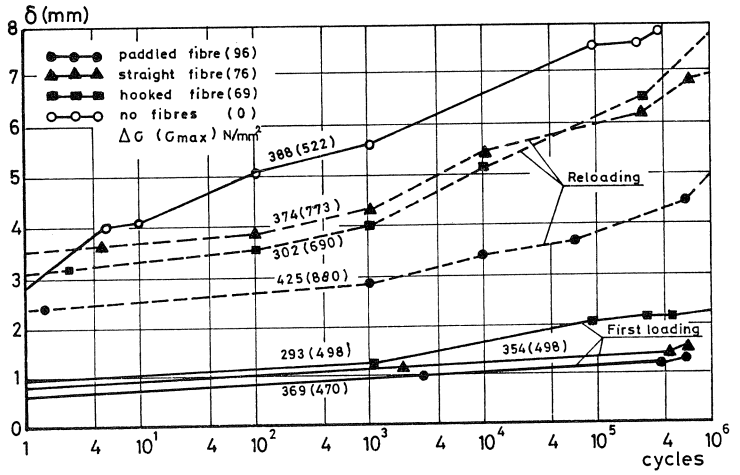

Fig. 3. Deflection-N curves for beams with 2 Ø 4 bars and steel fibres. σ and $\Delta\sigma$ are calculated without considering the contribution of the fibres.

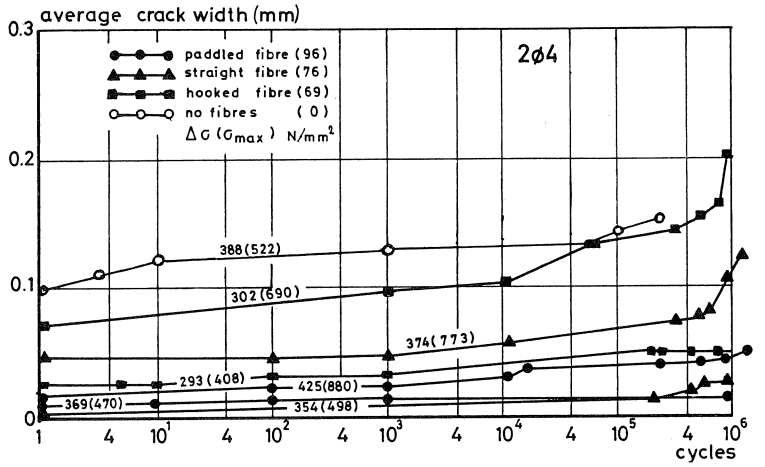

Fig. 4. Average crack width for beams with 2 Ø 4 bars during repeated loading.

- Test beams with 2 Ø4 reinforcement steel ($\rho = 0.17\%$) were subjected to a constant amplitude ($\Delta P = 0.35P$) fatigue loading with a maximum of about 50% of the static ultimate loading. Failure could be expected within two million cycles.
  In practice, none of the beams with fibres failed within one million cycles.
  The beams with fibres loaded with the same load showed only a very small increase in deflection (Fig. 3) - first cracks were hardly visible (Fig. 4).
  It was assumed that the cyclic load had not damaged the beams so that these same beams could be tested again using a higher maximum load (about $0.80P$) and the same amplitude as before (details in Table A2 of the Appendix). Now only the beams without fibres and with the lowest fibre volume failed. The failure was introduced by a failure of the reinforcement bars. Deflection and maximum crack width development is shown in Figs. 3 - reloading and 5, respectively.
  The stress data given in the figures will be discussed in chapter 5.
- Beams with 4 Ø 6 reinforcement steel were subjected to a constant amplitude ($\Delta P = 0.54P$) fatigue loading with a maximum of about 67% of the static ultimate loading. Only the beam with the highest fibre volume did not fail within 1.4 million cycles.
  The data are given in Table A2 in the Appendix. Deflections, average and maximum crack widths are shown in Figs. 6, 7 and 8.
- The last series with 4 Ø10 bars was tested with a constant amplitude of $\Delta P = 0{,}68P$ and a maximum of about 82% of the static ultimate loading.
  All the beams failed within one million cycles after about the same time (Table A2 in the Appendix). Deflection and crack width data are shown in Figs. 9, 10 and 11.
- The data about crack distances are summarized in Table A3 in the Appendix. Figs. 12 through 14 show photographs of the marked beams after the test, which give a clear impression of the crack distances.

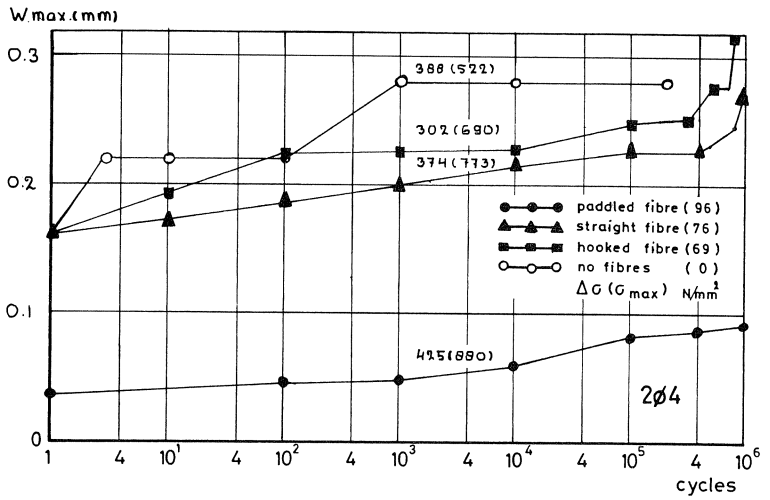

Fig. 5. Maximum crack width for beams with 2 Ø 4 bars during repeated loading.

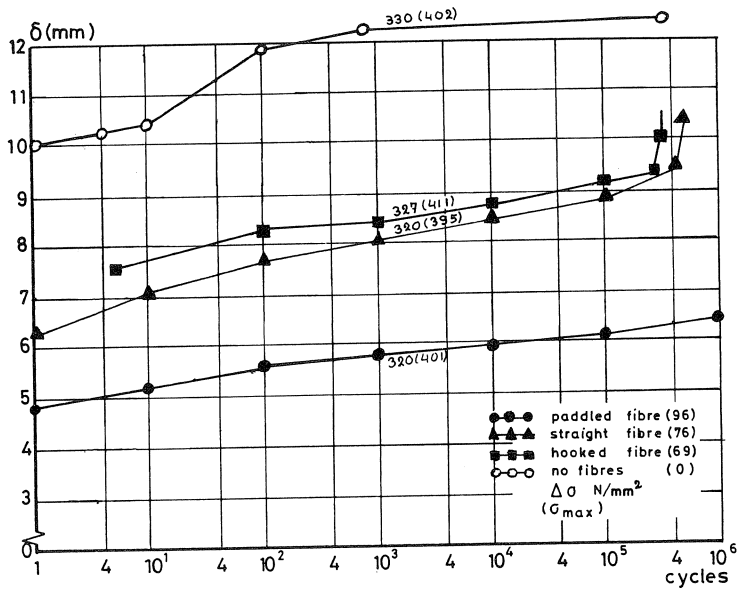

Fig. 6. Deflection-*N* curves for beams with 4 Ø 6 bars and steel fibres.

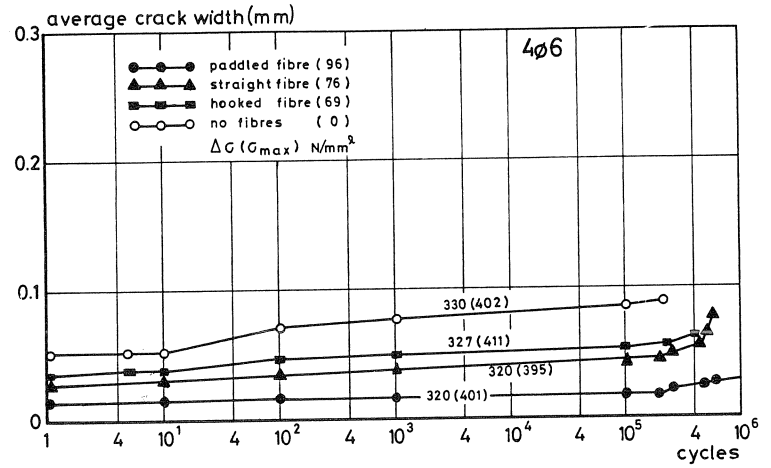

Fig. 7. Average crack width for beams with 4 Ø 6 bars during repeated loading.

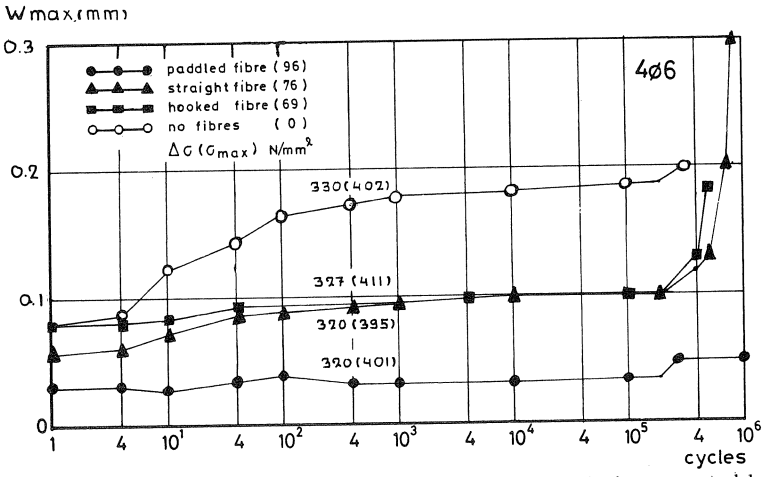

Fig. 8. Maximum crack width for beams with 4 Ø 6 bars during repeated loading.

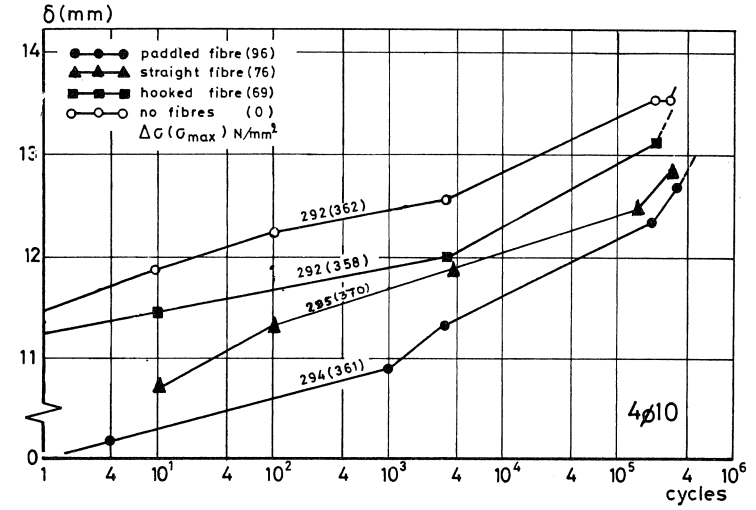

Fig. 9. Deflection-*N* curves for beams with 4 Ø10 bars and steel fibres.

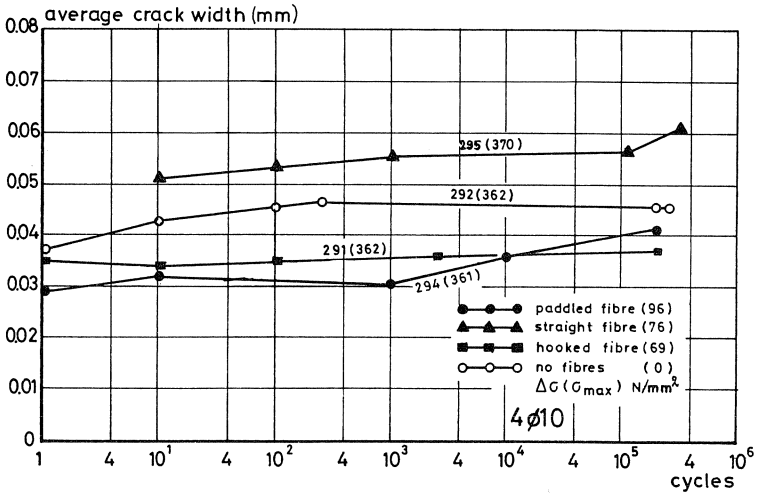

Fig. 10. Average crack width for beams with 4 Ø10 bars during repeated loading

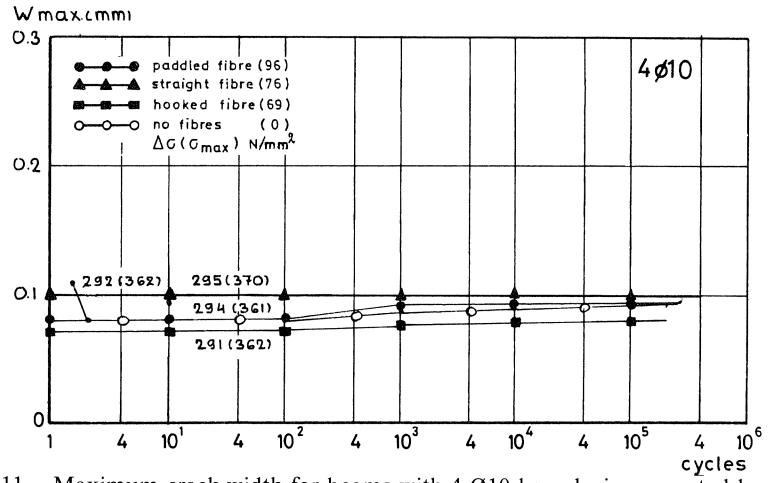

Fig. 11. Maximum crack width for beams with 4 Ø10 bars during repeated loading.

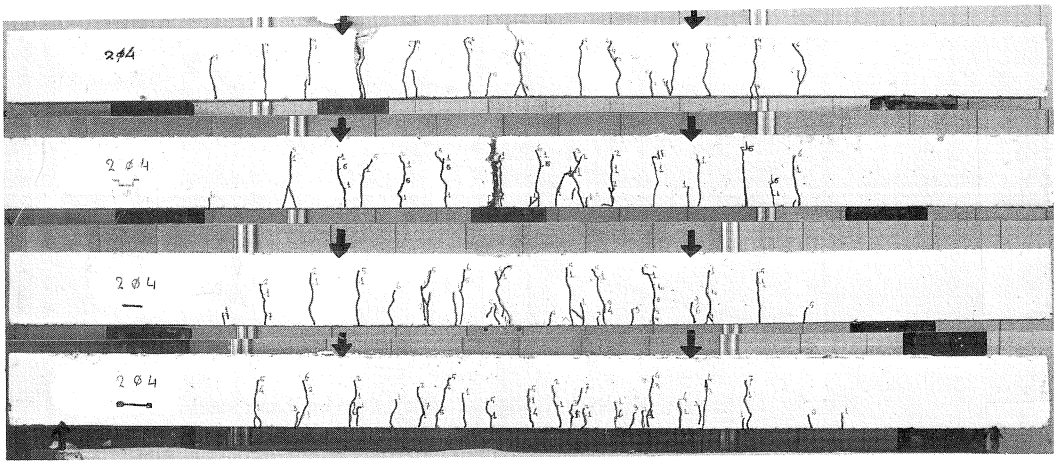

Fig. 12. Crack pattern of beams with 2 Ø 4 bars.

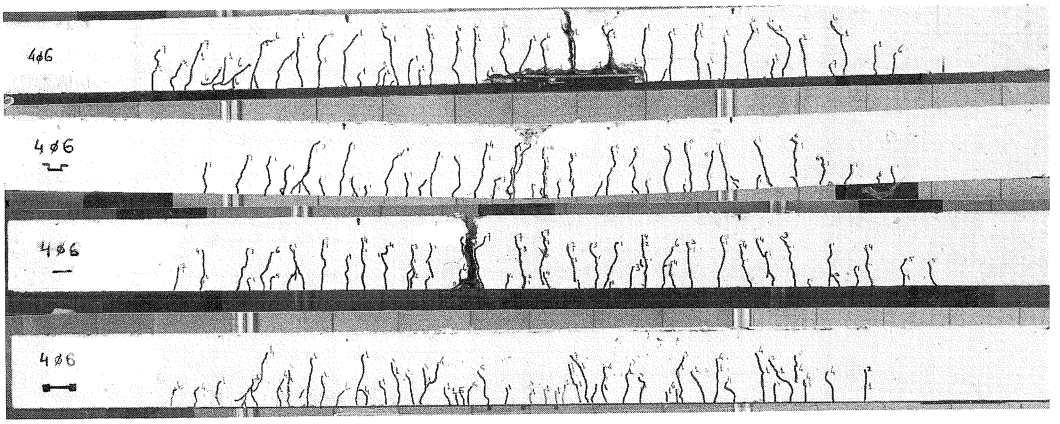

Fig. 13. Crack pattern of beams with 4 Ø 6 bars.

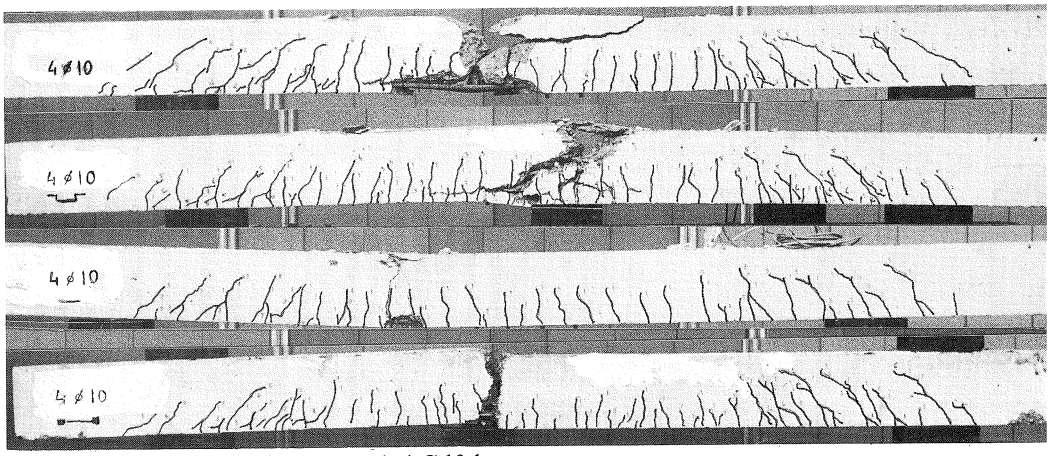

Fig. 14. Crack pattern of beams with 4 Ø 10 bars.

5 Discussion of the results

In the literature about fibre reinforced concrete, the "aspect ratio", i.e. the ratio between length and diameter of the fibre, is used for characterizing the mechanical properties of a particular fibre. As a measure for the properties of a group of fibres in the concrete, the volume aspect ratio (pl/d), i.e. the volume percentage of the fibres multiplied by the aspect ratio, seemed to be very advantageous in describing the influence of the fibres on the fatigue life of the beams. The Figs. 15, 16 and 17 show this parameter as a function of the number of cycles to failure. At each point in the figures the stress data of the par-

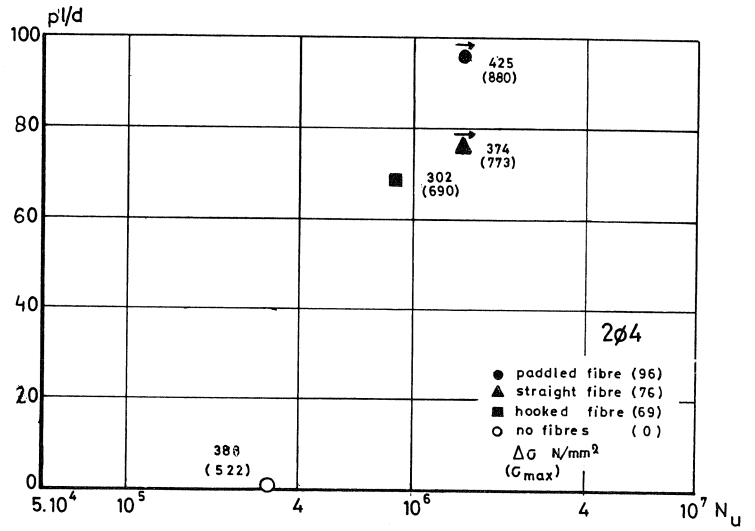

Fig. 15. Influence of the volume aspect ratio on the fatigue life of beams with 2 Ø 4 bars.

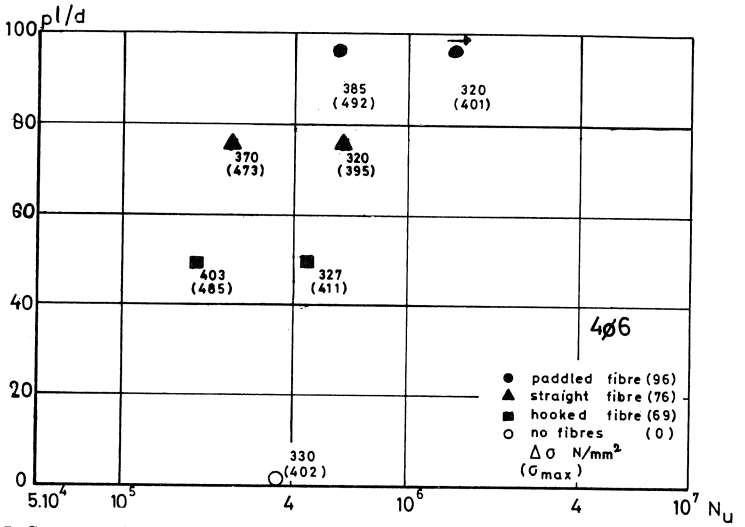

Fig. 16. Influence of the volume aspect ratio on the fatigue life of beams with 4 Ø 6 bars.

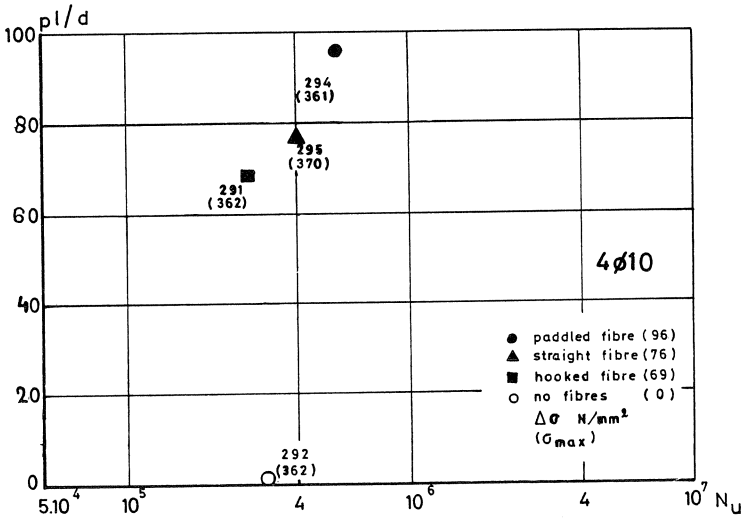

Fig. 17. Influence of the volume aspect ratio on the fatigue life of beams with 4 Ø10 bars.

ticular tests are given calculated in accordance with the cracked section elastic analyses. In these analyses the stresses in the reinforcement steel are calculated in the conventional way, ignoring the contribution of the fibres. Thus the stresses given in the figures are fictitious; on the other hand they show the influence of the fibres very well.

In the figures the number between parentheses is the maximum steel stress, the other one is the steel stress amplitude. It can be seen that the number of cycles till failure increases with an increasing pl/d ratio. This effect slowly diminishes if more bar reinforcement is present.

This result could be expected; if there is only a little bar reinforcement any additional reinforcement (for instance fibres) must have a significant effect, whereas this effect gets hidden where the concrete is already highly reinforced with bars.

In Fig. 16 on the left side, some results of additional tests not mentioned before are given to illustrate what happens if the maximum stress and amplitude will increase. They indicate a trend toward a lower number of cycles till failure.

This effect is valuable for all reinforcement ratios. To know the real behaviour of the fibres in the beams it is necessary to obtain the real steel stresses and the fibre stresses during the fatigue loading. Due to the fact that surface strain measurements at the bottom of the beams were very unreliable, these strains have been calculated from the deflection and top surface strain measurements. The method is described in the paper by Reinhardt in this HERON edition and will be summarized here shortly. The curvature is assumed to be $\kappa = 8\delta/l^2$ in which l = distance between the two outer deflection points and δ is the difference between centre deflection and outer deflection. The curvature κ is also a relation between the bottom and top surface strains, according to $\kappa = (\varepsilon_t + |\varepsilon_c|)/h$.

If κ is calculated from the deflection, h is known and ε_c is measured, then ε_t and ε_{steel} can be derived. With the stress-strain curves for the steel bars, the steel stresses and

steel forces are also known. Knowing these steel forces, the fibre contribution can be calculated from the equilibrium between internal and external moments.

This method for calculation of steel stresses seemed to be advantageous for medium and low reinforcement ratios. For high reinforcement ratios, however, the influence of the amount of steel bars in conjunction with the steel fibre amount was too great for a reliable fibre stress calculation. Rebar moment and external moment are of the same order now. The difference between both moments, i.e. the internal moment contribution of the fibres, becomes inaccurate, especially when the internal steel moment is not exactly known. Thus, only for beams with 2 Ø 4 or 4 Ø 6 bars the increasing of the steel bar contribution to the total moment results in a remarkable increase of the steel stresses. Fibres will be pulled out and are forced to transfer a part of their bearing capacity to

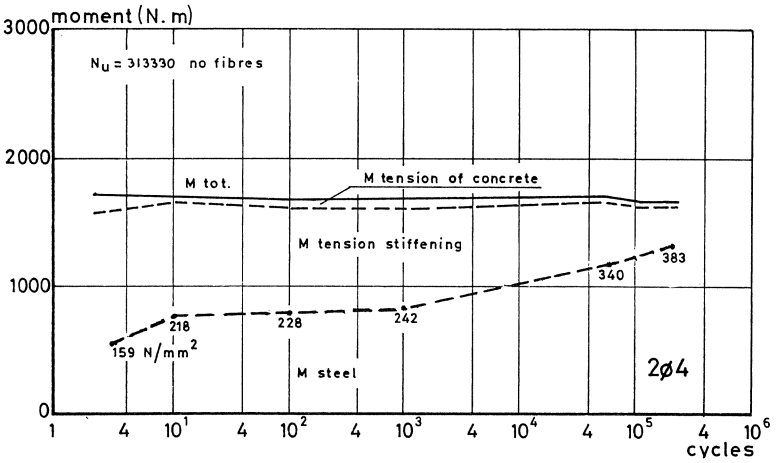

Fig. 18. Contribution to the moment in beams without fibres and with 2 Ø 4 bars during repeated loading.

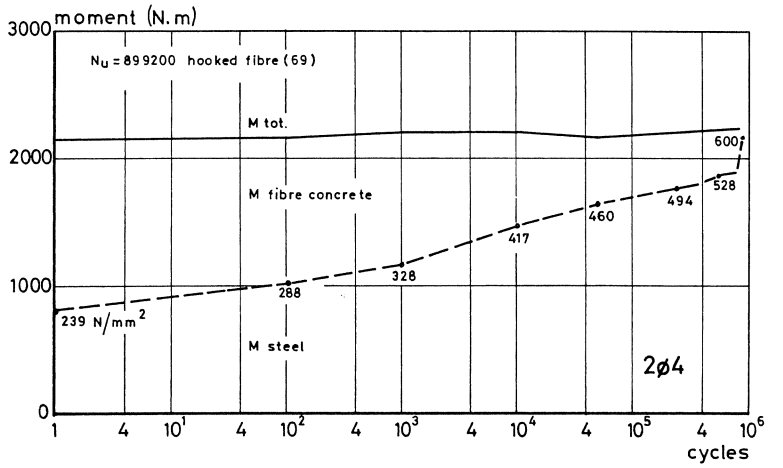

Fig. 19. Contribution to the moment in beams with hooked fibres and 2 Ø 4 bars during repeated loading.

the steel. Other influences responsible for an increase in steel stress are the dynamic creep in the compression zone and a decrease in tension stiffening in the tensile zone.

This is illustrated for beams with 2 Ø4 reinforcement in Figs. 18, 19, 20 and 21, and for 4 Ø6 beams in Figs. 22, 23 and 24. From the now "real" steel stresses can be seen that during the cyclic loading the steel stresses are growing slowly till just before the moment of failure. After a sudden increase of stress the reinforcing bars in the beams fail. As shown in Fig. 18 the contribution of the tension stiffening could be calculated. For fibre concrete however, it is not quite clear at this moment what is the order of the beneficial effect of the fibres on the tension stiffening. Tests have shown this effect, but it is still too early to draw conclusions. So the *M* fibre concrete contribution in Figs. 19 and so on consists also of a part tension stiffening which is not quantified.

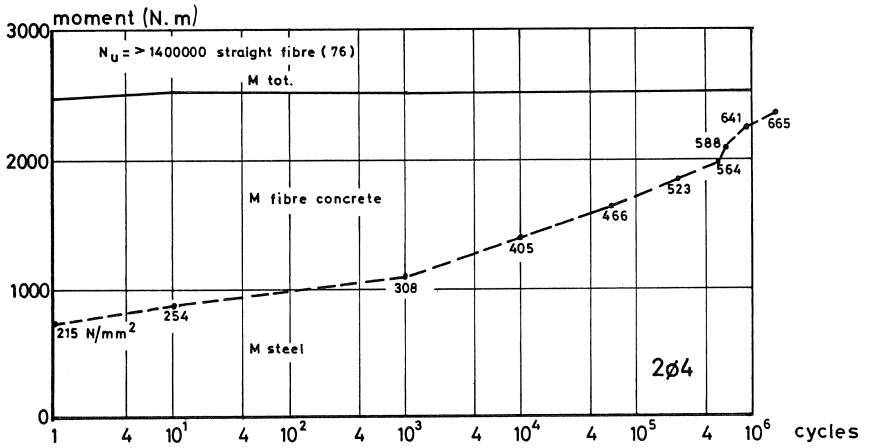

Fig. 20. Contribution to the moment in beams with straight fibres and 2 Ø 4 bars during repeated loading.

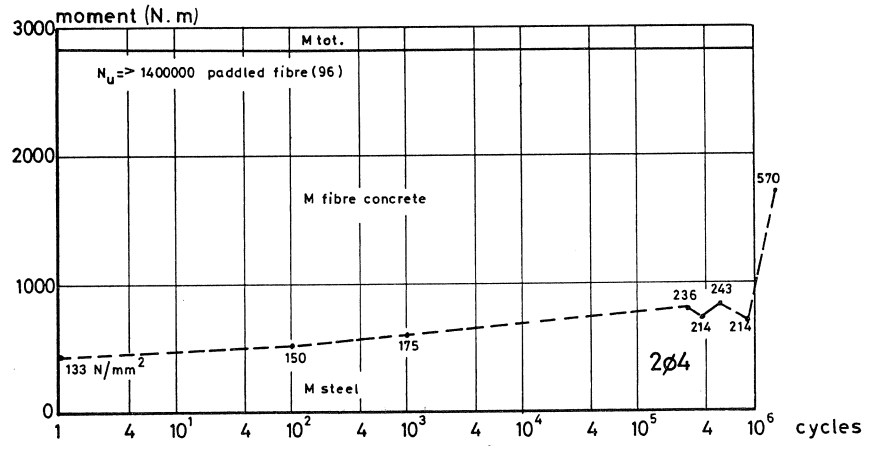

Fig. 21. Contribution to the moment in beams with paddled fibres and 2 Ø 4 bars during repeated loading.

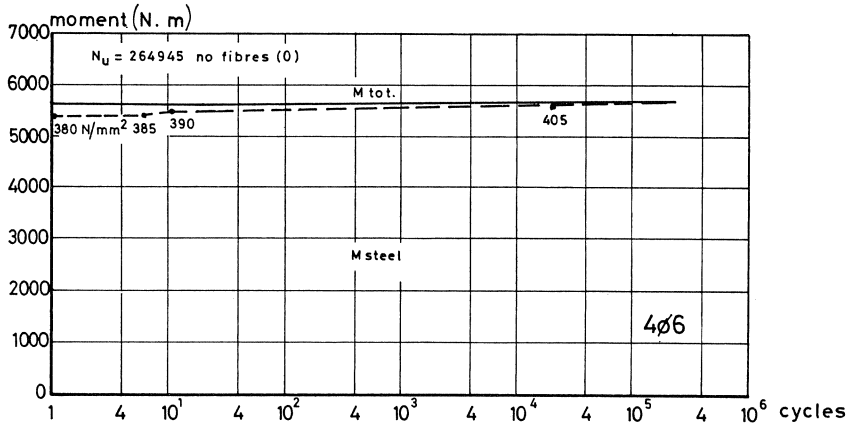

Fig. 22. Contribution to the moment in beams without fibres and 4 Ø 6 bars during repeated loading.

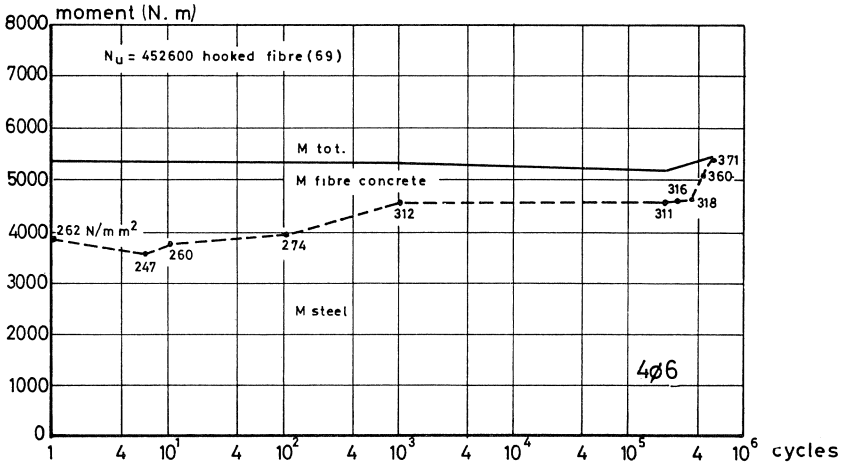

Fig. 23. Contribution to the moment in beams with hooked fibres and 4 Ø 6 bars during repeated loading.

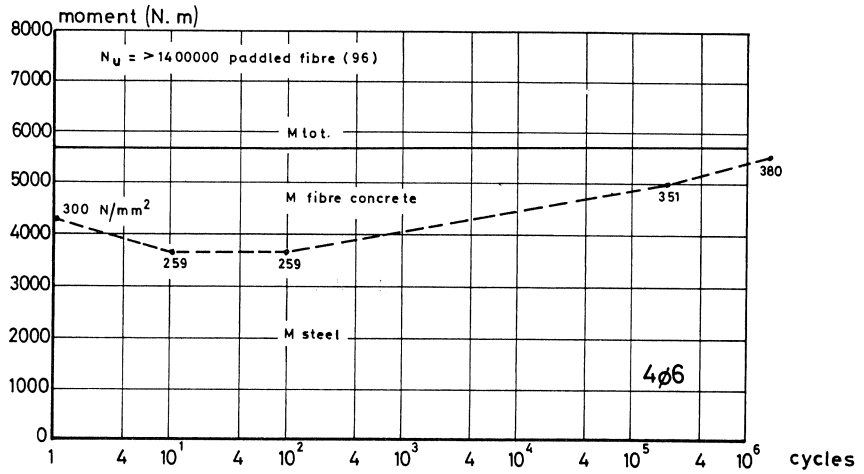

Fig. 24. Contribution to the moment in beams with paddled fibres and 4 Ø 6 bars during repeated loading.

Concerning crack width, plots are given for average and maximum crack width in relation to the *pl/d* ratio. The average crack width is illustrated in Figs. 25, 26 and 27 and the maximum crack width in the Appendix, Figs. A1, A2 and A3. The plots are taken after 10.000 cycles and so represent an intermediate state. For comparison the static crack width values are shown at the same stress levels. For all reinforcement ratios there is an increase in crackwidth after 10.000 cycles. The increase is larger for the lower *pl/d* values and the lower reinforcement ratios.

For instance, for the beams with a mean reinforcement ratio, i.e. the beams with 4 Ø6 bars (Fig. 26), the average crack width for the beams without fibres is for a steel stress of

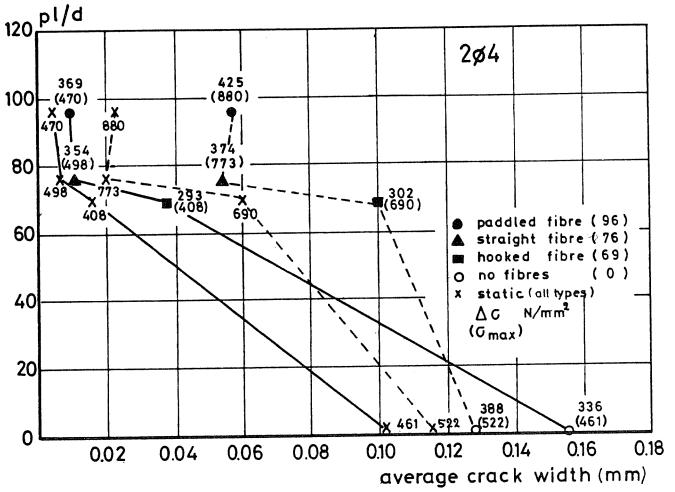

Fig. 25. *pl/d* vs average crack width for beams with 2 Ø 4 bars at 10000 cycles.

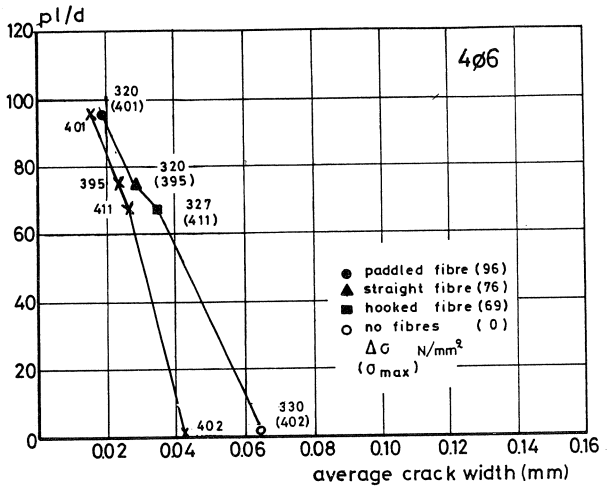

Fig. 26. *pl/d* vs average crack width for beams with 4 Ø 6 bars at 10000 cycles.

402 N/mm^2 0.043 mm. After 10.000 cycles this value has grown to 0.065 mm. For the same load the beam with the highest pl/d ratio shows in the static case an average crack width of 0.016 mm, which grows to 0.02 mm after 10.000 cycles. It is worth noting that even for the highest reinforcement ratios (4 Ø10 bars) where the fibres do not influence the strength, an influence of the fibres on the crack width is visible. This is due to the local influence of the fibres.

From the crack spacing it is known that it is commonly smaller with a greater reinforcement ratio. That is also the case as can be seen in Fig. 28 for $pl/d = 0$.

There the average crack spacing just before failure is about 95 mm for 2 Ø4 reinforced

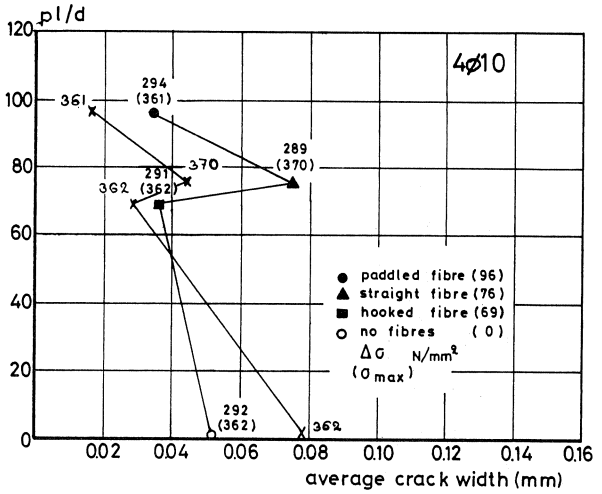

Fig. 27. pl/d vs average crack width for beams with 4 Ø 10 bars at 10000 cycles.

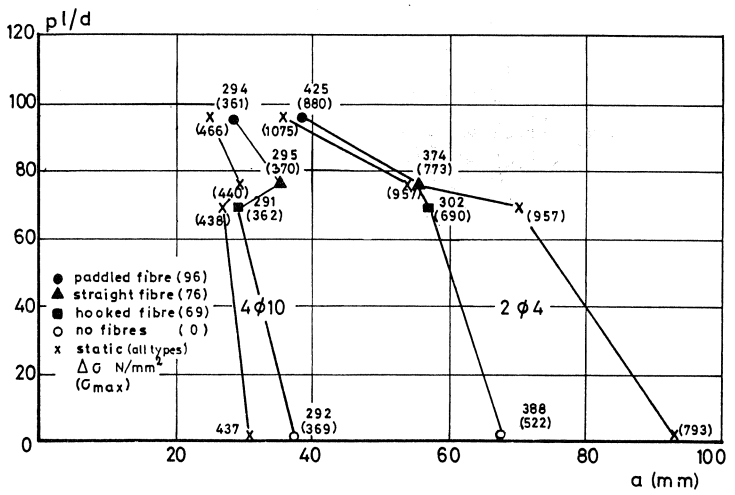

Fig. 28. Crack spacing a vs pl/d ratio for 2 Ø 4 and 4 Ø 10 reinforced beams.

beams and between 30 and 40 mm for 4 Ø10 reinforced beams in the static case.

The lower limit which is determined by the bond properties of the steel, the concrete quality and the geometry of the beam seems to be about 25 mm. This limit is not undercut, not even in the dynamic tests. Also for the higher reinforcement ratios there is hardly any influence of the fibres. Only at low reinforcement ratios both influences are evident: dynamic loading reduces the crack spacing, and the higher pl/d ratio reduces it as well to a considerable extent.

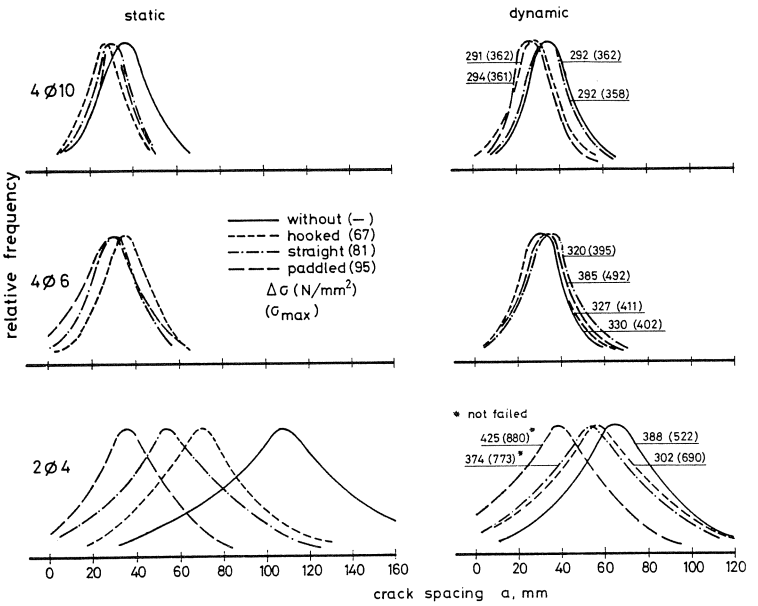

Fig. 29. Relative frequency of crack spacing in static and dynamic tests.

The influence of the reinforcement ratio shall be illustrated by a few more diagrams showing the frequency distribution of the crack spacing. On the lower part of Fig. 29, the distributions are rather different for the four cases of plain concrete and three types of fibres. It can be seen that the fibres contribute to the cracking behaviour at low reinforcement ratios. This effect is levelled at higher reinforcement ratios. That is true for the absolute value of the crack spacing and also for the scatter of the results. The right hand side gives the influence of dynamic loading. It can be seen that only for a low reinforcement ratio (2 Ø 4) the crack spacing decreases by dynamic loading, whereas for higher reinforcement ratios there is no obvious difference between static and dynamic behaviour.

It must be noted that the frequency diagrams of Fig. 29 are idealized, based on a normal distribution of the crack spacing which is not quite correct. However, this presentation shows the fibre influence in the best way.

6 Conclusions

It turned out that the volume aspect ratio pl/d is a suitable parameter in order to describe the various influences. It can be noted that fibre reinforcement increases the number of cycles to failure and diminishes the crack width, crack spacing and deflections for a given static load and for a given number of cycles.

The beneficial influence is more distinct the smaller the bar reinforcement ratio and the higher the pl/d ratio. It appears that the addition of fibres substantially reduces the average tensile stresses in the continuous bars. However, during fatigue loading the rebar stresses grow as a result of the debonding of the steel, dynamic creep of concrete in compression and pull-out behaviour of the fibres. Due to the same effects, deflections and crack widths also increase during cyclic loadings.

This behaviour depends on the absolute level of the steel stresses and can only occur if a certain stress level is reached. More research is needed in order to determine this stress level exactly.

7 Notation*

a	crack spacing
b	depth of beam
d	diameter of fibre
h	height of beam
l	length of fibre
p	volume percentage of fibres
pl/d	volume aspect ratio
w	crack width
M	moment
N_u	number of cycles till failure
P	static ultimate load
ΔP	load amplitude
δ	deflection
ε_c	compression strain concrete
ε_t	tension strain concrete
ε_s	tension strain steel
ρ	bar reinforcement ratio
σ	steel stress
$\Delta\sigma$	steel stress amplitude
κ	curvature

* Notation is given here as far as it does not follow clearly from the text.

8 Appendix

Table A1. Scope of beam tests.

fibres	bar reinforcement $\rho = 0.17\%$ (2 Ø 4)	$\rho = 0.75\%$ (4 Ø 6)	$\rho = 2.09\%$ (4 Ø 10)
none	x	x	x
hooked	x	x	x
straight	x	x	x
paddled	x	x	x

Table A2. Fatigue data of beams.

bar reinforcement	type of fibre	P_{min}* (N)	P_{max}* (N)	$\frac{P_{max}}{P_{ult}}$*	number of cycles to failure	remarks
2 Ø 4	none	1414	5510	.75	313330	
	hooked	1214	4306	.49	$> 1.2 \times 10^6$	
		4093	7283	.82	899200	reloaded
	straight	1520	5256	.55	$> 1.4 \times 10^6$	
		4211	8159	.85	$> 1.4 \times 10^6$	reloaded
	paddled	1066	4961	.41	$> 1.4 \times 10^6$	
		4802	9288	.77	$> 1.4 \times 10^6$	reloaded
4 Ø 6	none	3420	19096	.72	264945	
	hooked	3990	19523	.73	452606	
	straight	3563	18763	.60	600380	
	paddled	3848	19048	.63	1.4×10^6	
4 Ø 10	none	9236	47765	.85	310900	
	hooked	9369	47765	.84	264810	
	straight	8709	47237	.83	238810	
	paddled	8840	47633	.78	540000	

* Loads do not include dead weight.

Table A3. Crack distances in dynamic tests.

bar reinforcement	fibre type	mean value with 90% conf. interval (mm)
2 Ø 4	none	66.15 ± 45.60
	hooked	56.68 ± 52.80
	straight	54.22 ± 50.90
	paddled	38.03 ± 42.80
4 Ø 6	none	31.47 ± 21.70
	hooked	31.47 ± 24.20
	straight	36.54 ± 26.90
	paddled	32.81 ± 25.50
4 Ø 10	none	36.70 ± 23.04
	hooked	28.34 ± 22.95
	straight	35.10 ± 12.88
	paddled	27.59 ± 19.13

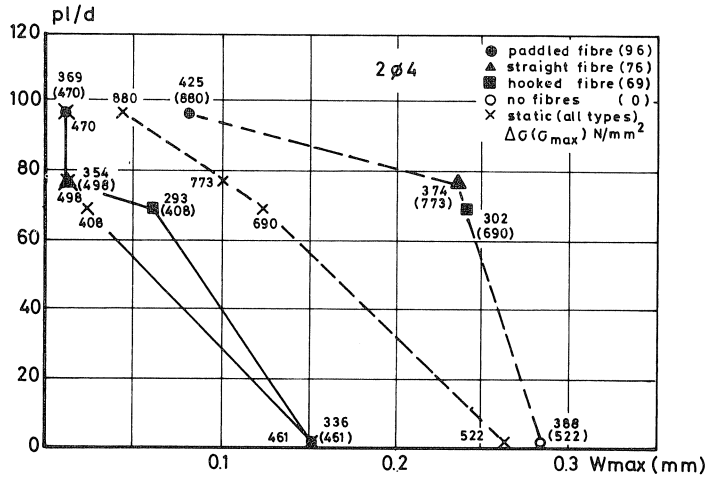

Fig. A1. *pl/d* vs maximum crack width for beams with 2 Ø 4 bars at 10000 cycles.

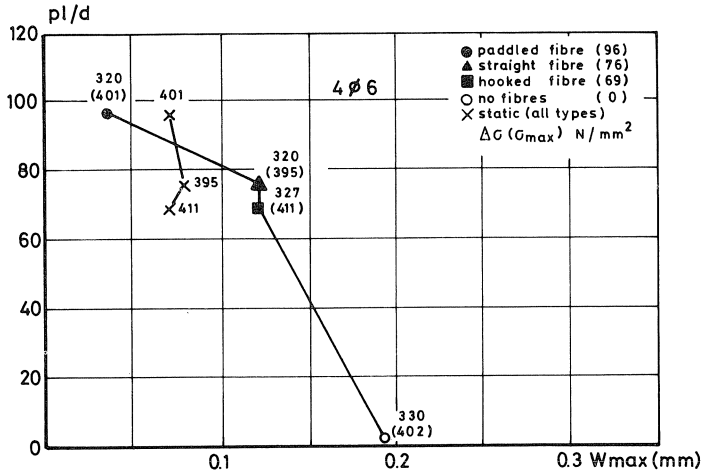

Fig. A2. *pl/d* vs maximum crack width for beams with 4 Ø 6 bars at 10000 cycles.

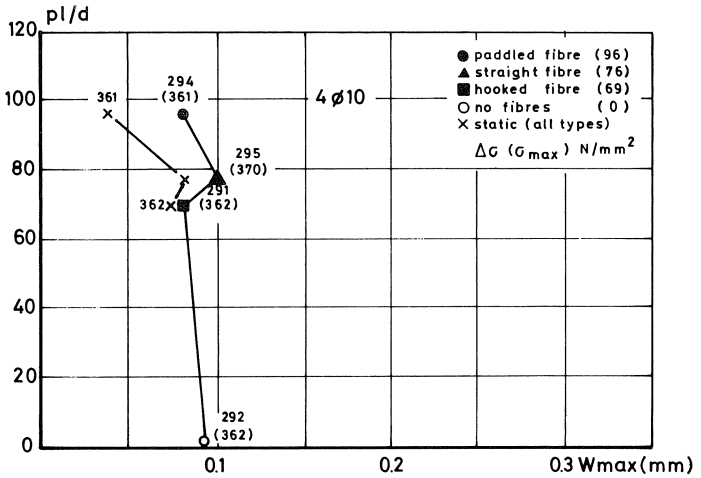

Fig. A3. *pl/d* vs maximum crack width for beams with 4 Ø 10 bars at 10000 cycles.